Title
USP15 regulates dynamic protein–protein interactions of the spliceosome through deubiquitination of PRP31

Journal
Nucleic Acids Research, 45(8)

ISSN
0305-1048

Authors
Das, Tanuza
Park, Joon Kyu
Park, Jinyoung
et al.

Publication Date
2017-05-05

DOI
10.1093/nar/gkw1365

Peer reviewed

4866–4880 *Nucleic Acids Research, 2017, Vol. 45, No. 8* *Published online 14 January 2017*
doi: 10.1093/nar/gkw1365

USP15 regulates dynamic protein–protein interactions of the spliceosome through deubiquitination of PRP31

Tanuza Das[1], Joon Kyu Park[2], Jinyoung Park[1], Eunji Kim[2], Michael Rape[3,4], Eunice EunKyeong Kim[2,*] and Eun Joo Song[1,*]

[1]Molecular Recognition Research Center, Korea Institute of Science and Technology, Hwarangno 14-gil 5, Seongbuk-gu, Seoul 02792, Korea, [2]Biomedical Research Institute, Korea Institute of Science and Technology, Hwarangno 14-gil 5, Seongbuk-gu 02792, Seoul, Korea, [3]Department of Molecular and Cell Biology, University of California, Berkeley, CA 94720, USA and [4]Howard Hughes Medical Institute, University of California, Berkeley, Berkeley, CA 94720, USA

Received June 05, 2016; Revised December 26, 2016; Editorial Decision December 27, 2016; Accepted January 02, 2017

ABSTRACT

Post-translational modifications contribute to the spliceosome dynamics by facilitating the physical rearrangements of the spliceosome. Here, we report USP15, a deubiquitinating enzyme, as a regulator of protein–protein interactions for the spliceosome dynamics. We show that PRP31, a component of U4 snRNP, is modified with K63-linked ubiquitin chains by the PRP19 complex and deubiquitinated by USP15 and its substrate targeting factor SART3. USP15^{SART3} makes a complex with USP4 and this ternary complex serves as a platform to deubiquitinate PRP31 and PRP3. The ubiquitination and deubiquitination status of PRP31 regulates its interaction with the U5 snRNP component PRP8, which is required for the efficient splicing of chromosome segregation related genes, probably by stabilizing the U4/U6.U5 tri-snRNP complex. Collectively, our data suggest that USP15 plays a key role in the regulation of dynamic protein–protein interactions of the spliceosome.

INTRODUCTION

Pre-mRNA splicing is catalyzed by one of the most complex and dynamic macromolecular machines called the spliceosome which is assembled from five small nuclear RNAs (snRNAs) and numerous proteins. This large ribonucleoprotein (RNP) is assembled onto intron-containing mRNAs by the recognition of the 5′ splice site by U1 snRNP and the branch point by U2 snRNP (1,2). Upon formation of the A complex, the U4/U6.U5 tri-snRNP complex is recruited to generate the B complex. After rearrangements in RNA-RNA and RNA-protein interactions, the U1 and U4 snRNAs and their associated proteins are released yielding the catalytically activated spliceosome. The activated spliceosome then catalyzes the excision of introns and the ligation of exons. As such, the spliceosome undergoes rapid but tightly regulated changes in its composition during its catalytic cycle, with distinct proteins and RNAs associating and dissociating at defined stages of the splicing reaction (3,4). Proper pre-mRNA splicing is one of the most critical steps in gene expression, and defects in splicing are well known as a common disease-causing mechanism in humans (5). Although the detailed mechanism is not yet known, cell cycle progression is closely related to RNA splicing. For example, splicing regulators like SON and SR factor have been shown to contribute to the precise splicing of cell cycle regulators (6–9). Moreover, recently, it has been reported that many genes undergo cell cycle dependent alternative splicing changes and that periodic alternative splicing is controlled by CLK1 (10).

Post-translational modifications contribute to the spliceosome dynamics by facilitating the physical rearrangements of the spliceosome (4,11–13), for example, phosphorylation has an important role in the regulation of the spliceosome (12,14). Ubiquitin modification is involved in diverse cellular processes such as protein degradation, regulation of cellular activity, localization and interaction (15). Ubiquitin has seven lysine residues, K6, K11, K27, K29, K33, K48 and K63 which result in the formation of polyubiquitin chains. These chains are diverse in structure and function depending on the lysine residue used. For instance, K11- or K48-linked chains promote degradation of ubiquitinated proteins by 26S proteasome (16). On the other hand, K63-linked chains are not responsible for proteolysis. Instead, they regulate protein localization and assemble of DNA repair complexes as well as are involved in signal transduction or kinase activation (17,18). Recently, reversible ubiquitination has been shown to have a critical role in regulating the spliceosome dynamics.

*To whom correspondence should be addressed. Tel: +82 2 958 5086; Fax:+ 82 2 958 5170; Email: ejsong@kist.re.kr
Correspondence may also be addressed to Eunice EunKyeong Kim. Tel: +82 2 958 5937; Fax: +82 2 958 5909; Email: eunice@kist.re.kr

For example, it has been shown in yeast extracts that ubiquitination is required to assemble and disassemble the U4/U6.U5 tri-snRNP complex through ubiquitin conjugation of PRP8 which is a component of the U5 snRNP (11). Also we have reported that the modification of PRP3, which is a component of the U4 snRNP, with K63-linked ubiquitin chains by the PRP19 complex and USP4 with its substrate targeting factor SART3 guides the rearrangement of the complex resulting in an active spliceosome, and the loss of USP4 impairs mitotic progression by interfering with mRNA splicing, for example, of α-tubulin and Bub1 (19).

Because the spliceosome consists of >100 proteins and needs tight regulation for its dynamics, we thought that other proteins beside PRP3 might be reversibly modified by ubiquitination and deubiquitination. Therefore, we have been screening for other spliceosomal proteins that require ubiquitin-dependent regulation in mitotic progression. Here, we report that PRP31, which is a component of the U4 snRNP, is another spliceosomal protein. It is modified with K63-linked ubiquitin chains by the PRP19 complex and deubiquitinated by USP15 and its substrate targeting factor SART3. SART3 mediates complex formation with USP15 and USP4, and this complex leads to simultaneous deubiquitination of the substrates PRP31 and PRP3. In addition, the depletion of USP15 and USP4 interferes with proper mRNA splicing of Bub1 and α-tubulin and chromosome segregation. We propose that PRP31 and PRP3 serve as regulatory proteins in the rearrangements of the spliceosome components by reversible ubiquitination and deubiquitination.

MATERIALS AND METHODS

Cell culture and transfections

HeLa and HEK 293T cells were maintained in Dulbecco's modified Eagle's medium (DMEM) supplemented with 10% heat inactivated fetal bovine serum, penicillin (10 U/ml) and streptomycin (100 μg/ml). All cells were incubated at 37°C in 5% CO_2. Plasmids were transfected in HEK 293T cells, using the calcium phosphate/DNA coprecipitation method (20). Transfection in HeLa cells was performed with the Effectene transfection reagent (Qiagen) according to the manufacturer's instructions.

Cloning and antibodies

USP15 and PRP31 genes were amplified by PCR and cloned into the pCS2 expression plasmid, incorporating HA, Myc or Flag tag on the N terminus. The catalytically inactive mutant of $USP15^{C269A}$ was made by mutating the Cysteine (TGT) at position 269 into an Alanine (GCT) using a site directed mutagenesis kit (Stratagene). For $USP15^{U4L1}$ and $USP15^{U4L2}$, linker 1 (amino acid 223–255) and linker 2 (amino acid 441–758) of USP15 were swapped with linker 1 (amino acid 227–297) and linker 2 (amino acid 483–777) of USP4, respectively. Deletion mutants of USP15, SART3 and PRP31 were generated by PCR and cloned into the same vectors as described. Ubiquitin and various mutants were cloned into pCS2 for expression in human cells (11,16).

The following antibodies were purchased and used for immunostaining and western blotting: antibodies against USP15 (Bethyl Laboratories Inc.), USP4 (Bethyl Laboratories Inc.), SART3 (Bethyl Laboratories Inc.), β-actin (Santa Cruz Biotechnology Inc.), Myc (Santa Cruz Biotechnology), HA (Santa Cruz Biotechnology), Flag (Sigma-Aldrich), PRP31 (Sigma-Aldrich) and Alexa-488 or Alexa-546 conjugated secondary antibodies (Invitrogen).

Protein purification and gel filtration chromatography

The human SART3 HAT domains (residues 1–691) and DUSP-UBL domain of USP15 (residues 1–226) were cloned into pET-28a (Novagen) to generate N-terminal histidine-tagged proteins. The N-domain (residues 1–333) and C-domain (residues 85–499) of human PRP31 were cloned into pET-32a (Novagen) as N-terminal histidine-tagged thioredoxin fusion proteins. All proteins were expressed in *Escherichia coli* Rosetta (DE3) cells with induction by 0.5 mM isopropyl-β-D-thiogalactoside at 18°C for 18 h. Proteins in 50 mM Tris–HCl (pH 8.0) and 150 mM NaCl buffer were purified with His-Trap affinity column (GE Healthcare) eluted with 25–500 mM imidazole. Affinity tags were removed with thrombin, and the resultant proteins were then further purified with a Superdex 200 26/60 gel filtration column (GE Healthcare) which had been pre-equilibrated with 50 mM Tris–HCl (pH 8.0) and 150 mM NaCl.

For the separation of protein complexes, cell lysates over-expressed with HA-SART3, Myc-USP4 and Flag-USP15 were co-fractionated by gel filtration with a Superdex 200 10/300 column (GE Healthcare) in a buffer containing 50 mM Tris–HCl (pH 7.4), 150 mM NaCl and 1 mM EDTA. Molecular weight markers (Sigma-Aldrich) with a range of 66 000–443 000 Da were used for size calibration. Eluted fractions (0.5 ml) were collected and aliquots were subject to the SDS-PAGE and detected by western blotting.

GST pull down assay

GST-$USP15^{1–226}$ and GST-$USP4^{1–230}$ were coupled to glutathione beads (Sigma) and incubated with $SART3^{1–691}$ for 3 h at 4°C. Beads were washed with buffer containing 50 mM HEPES, pH 7.5, 150 mM NaCl, 1.5 mM $MgCl_2$, 5 mM KCl and 0.1% Tween-20, and eluted with 2× SDS sample buffer. Samples were separated by SDS-PAGE and detected by Coomassie staining.

siRNA knockdown experiments

Three different siRNAs targeting three different regions of the USP15 gene were used for the knockdown. USP15-1 (5′-CUAUGGAAAUGAUGAAG-3′) was designed to target the 3′ UTR region of USP15, whereas USP15-2 (5′-AGGAAUGAGAGGUGAAAUA-3′) and USP15-3 (5′-GCAGAUAAGAUGAUAGUUA-3′) targeted the ORF region.

The siRNA sequences used were 5′-CGAAGAAUGGAGAGGGAACA-3′ for USP4, and 5′-GGAGACAGGAAAUGCCUUA-3′ and 5′-GAUGUGGUGUCCUGAGAUA-3′ for SART3.

The siRNA sequence for the negative control was 5′-CCUACGCCACCAAUUUCGU-3′ which was used as a mock transfection. All the siRNAs were transfected into HeLa cells with Lipofectamine 2000 (Invitrogen) according to the manufacturer's instructions. Cells were harvested 48 h after the transfection.

His-ubiquitin pull-down assay

HeLa cells were transfected with pCS2-His-ubiquitin and pCS2-tagged constructs as indicated. Nocodazole was added to cells 24 h after transfection to a concentration of 100 ng/ml. Twenty-four hours after nocodazole treatment, cells were resuspended in Buffer A (6 M guanidine–HCl, 0.1 M Na_2HPO_4/NaH_2PO_4, 10 mM imidazole, pH 8.0) and sonicated. Cell lysates were added to 50 μl of equilibrated Ni-NTA agarose followed by incubation for 4 h at room temperature. Beads were then washed twice with Buffer A, followed by two washes with Buffer A/TI (1 vol of Buffer A, 3 vol of Buffer TI (25 mM Tris–Cl, 20 mM imidazole at pH 6.8)), and finally one wash with Buffer TI. The protein conjugates were eluted in 30 μl 2× laemmli/imidazole (200 mM imidazole) and boiled at 95°C for 10 min. Elutes were analyzed by western blotting. Even though Ni-pull down was performed under denaturing condition, unmodified proteins could also be purified in the pull down assay. The unmodified proteins might be a result from short histidine tracks in the proteins or property of proteins to bind metals in IMAC (21).

Immunoprecipitation

Transfected HEK 293T or HeLa cells were harvested and lysed in IP buffer (50 mM HEPES, pH 7.5, 150 mM NaCl, 1.5 mM $MgCl_2$, 5 mM KCl, 0.1% Tween-20, 2 mM DTT and protease inhibitor cocktail (Roche)). For single IP, lysates were centrifuged at 12 000 rpm for 30 min at 4°C and supernatants were incubated with anti-HA (Sigma) or anti-Flag M2 agarose (Sigma) beads for 4 h at 4°C. For sequential IPs, cell lysates were immunoprecipiated with anti-Flag M2 agarose beads (Sigma) and then incubated with 100 mg/ml 3× FLAG peptide (Sigma) in lysis buffer. After elution with the FLAG peptide, eluted samples were used for the second IP by anti-HA beads (Sigma). Beads were washed with buffer containing 50 mM HEPES, pH 7.5, 150 mM NaCl, 1.5 mM $MgCl_2$, 5 mM KCl, 0.1% Tween-20 and 2 mM DTT and eluted with 2× SDS sample buffer. Samples were analyzed and detected by western blotting.

Immunofluorescence analysis

HeLa cells were seeded on coverslips and transfected with plasmids. After 48 h, cells were fixed with 4% formaldehyde, and incubated with anti-HA (Santa Cruz Biotechnology) or anti-Myc (Santa Cruz Biotechnology) antibody, followed by secondary goat anti-rabbit antibody coupled to Alexa488 (Invitrogen) and goat anti-mouse antibody coupled to Alexa546 (Invitrogen). The nucleus was stained with DAPI (Invitrogen). Coverslips were mounted and fluorescence was visualized with 40× magnification on a confocal laser scanning microscope (Carl Zeiss, Inc.), and pictures were analyzed with the ZEN 2009 software.

To count cells with mitotic defects, HeLa cells grown on coverslips were transfected with the indicated siRNA and plasmids for subsequent rescue. After fixation and permeabilization, cells were stained with monoclonal anti-β-tubulin-Cy3™ (Sigma) for 2 h, and the nucleus was counterstained with DAPI. Cells with mitotic defects were counted at 40× magnification with a fluorescence microscope (Nikon eclipse TE 2000-U).

Isothermal titration calorimetry (ITC)

ITC measurements were done with a MicroCal iTC200 (MicroCal, Northampton, MA, USA) at 25°C, and the data were analyzed with the program ORIGIN 7.0. Protein samples were prepared in 50 mM Tris–HCl (pH 8.0) and 150 mM NaCl buffer. For binding of USP15 and SART3, the purified DUSP-UBL domain of USP15 was concentrated to 0.4 mM while the SART3 HAT domain was concentrated to 0.02 mM with a Vivaspin concentrator (Vivaspin, Satorious). In the case of the SART3 and PRP31 binding experiment, the purified SART3 HAT domain was concentrated to 0.2 mM and the N- and C-domains of PRP31 were concentrated to 0.01 mM.

Quantitative real time PCR analysis

RNA was isolated from nocodazole treated mitotic arrested HeLa cells followed by knockdown of the indicated genes by siRNA transfection (oligofectamine). RNA isolation was performed with the RNeasy® mini kit (Qiagen). One microgram of total RNA sample was reverse transcribed in a final volume of 20 μl using the Thermo Scientific DyNAmo cDNA Synthesis Kit with a random hexamer primer set. cDNA samples were diluted 20-fold and qPCR reactions were done with 2× SYBR Green/Rox Master Mix (Thermo Scientific), 200 nM primers and 100 ng of RNA. The experiments were done in triplicate for each data point, and the relative quantification in gene expression was determined with the $2^{\Delta\Delta Ct}$ method.

When primers were designed for qPCR, amplification of both spliced (matured) and nonspliced (immature) mRNA was taken into consideration. To amplify the region of spliced mRNA, primers were designed to anneal the exon junction with the exception of H2AX, which does not possess introns. Primers used to amplify the spliced gene were as follows: Bub1-F (Ex), CCATCAAGCCCAAGAC TGAA; Bub1-R (Ex), TTTAGCATCATTCAGATCTC CCT; α-tubulin-F (Ex), CTTACCTCGACTCTTAGCTT GTC; α-tubulin-R (Ex), GGATGGAGATGCACTCACG; H2AX-F, TCCCTTCCAGCAAACTCAAC and H2AX-R, TCCAGTTCAGAAGCCAACG. On the other hand to amplify intron containing nonspliced mRNA, primers were designed to anneal to an exon as well as its neighboring intron. Primers used to amplify a nonspliced gene were as follows: Bub1-F (Ex), GAGATGCTCAGCAACA AAC; Bub1-R (In), GACCACCTCAAACTACCTAG; α-tubulin-F (Ex) ACTTGGAACCCACAGTCATT and α-tubulin-R (In) TGGAGGAGGGAGAGA AGGAC.

RESULTS

USP15 functions in the regulation of chromosome segregation

Previously, we reported that USP4 is a deubiquitinating enzyme (DUB) that regulates the activity and the composition of the spliceosome (19). Among the 100 or so DUBs identified in humans, USP15 and USP11 are the only two that have the same domain architecture as USP4 (22,23) and they share sequence identities of about 60 and 49% with USP4. It is worth noting that the sequence homology of the DUSP-UBL domains of USP4 and USP15 is higher than that of the catalytic domain (Supplementary Figure S1). Because proteins with high sequence homology often have similarities in function, we investigated whether USP15 has any role in the regulation of mitosis.

To identify the function of USP15, siRNA for USP15 was transfected into HeLa cells, and a mitotic phenotype was observed after immunostaining with Cy3 labeled anti-β-tubulin. The depletion of USP15 using three different siRNAs targeting three different regions of the USP15 led to chromosome missegregation and defects in the spindle structure (Figure 1A, Supplementary Figure S2). In rescue experiments using siRNA-resistant USP15, the spindle defect was rescued by expression of USP15 wild type but not by the catalytically inactive $USP15^{C269A}$ (Figure 1B and C). These results show that DUB activity is required for the role of USP15 in the control of chromosome segregation. Because depletion of USP4 resulted in spindle checkpoint bypass in the presence of taxol (19), we calculated the mitotic index after co-depletion of USP4 and USP15. Depletion of USP4 or USP15 led to spindle checkpoint bypass, and co-depletion of both exhibited a slightly stronger phenotype (Figure 1D). These data suggest that USP15 and USP4 are involved in the same cellular pathway.

USP15 interacts with SART3

SART3, a U4/U6 recycling factor, has been shown to be a substrate targeting factor of USP4 (19,24,25). SART3 shuttles USP4 into the nucleus by nuclear localization sequence (NLS) (26), and is associated with USP15 to regulate H2B deubiquitination (27). The interaction analysis showed that USP4 and SART3 form a complex with the majority of the U4/U6-snRNP components such as PRP31, PRP3 and PRP4 (28). Based on these facts, we hypothesized that SART3 may serve as a substrate targeting factor for both USP15 and USP4, and we examined the mitotic phenotype by the depletion of SART3. Similar to USP15, the depletion of SART3 led to chromosome missegregation and spindle defects (Supplementary Figure S3). These results suggest that SART3 is also associated with chromosome segregation. In previous studies, the interactions between the purified truncation proteins of USP15 and SART3 were analyzed with isothermal titration calorimetry (ITC) and it is confirmed that the DUSP-UBL domain of USP15 interacts with the HAT-C domain of SART3 *in vitro* (26,29). Therefore, the interaction between SART3 and USP15 in the cells was examined. The result from the coimmunoprecipitation of USP15 with SART3 (Supplementary Figure S4A) was consistent with a previous report (27). The GST-pull down assay with the indicated purified proteins showed that the DUSP-UBL domain of USP15 directly interacted with SART3 (Supplementary Figure S4B) similar to what was shown earlier (26,29). Next, to confirm that the residues 1–226 of USP15 are sufficient for SART3 binding, we constructed truncations of USP15, $USP15^{1–226}$ and $USP15^{230–952}$ and performed immunoprecipitation. As shown in Supplementary Figure S4C, SART3 interacted with $USP15^{1–226}$ but not with $USP15^{230–952}$. Taken together, these data show that USP15 interacts with SART3 directly through the DUSP-UBL domains. To identify the regions of SART3 responsible for the interaction with USP15, HA tagged SART3 mutants were transiently overexpressed and immunoprecipitated (Supplementary Figure S4D). Similar to the previous reports (26,29), the result shows that the residues 286–440 of SART3 in HAT-C were required for the interaction with USP15 (Supplementary Figure S4E).

PRP31 is a substrate of USP15

Earlier, Song *et al.* performed siRNA screening to see whether the depletion of spliceosomal proteins results in similar mitotic defects as does loss of USP4 (19). The result showed that the loss of PRP4, PRP4B kinase, PRP31, USP39 and Lsm2 induce mitotic defects. Since the depletion of USP15 shows similar mitotic defects, we thought that those spliceosomal proteins might be the substrates of USP15 and tested whether they are a potential substrate of USP15. As shown in Figure 2A and Supplementary Figure S5, only PRP31 showed high-molecular-weight forms in the presence of ubiquitin which were significantly decreased by coexpression with USP15, while PRP8, PRP4, PRP4B kinase and USP39 did not. We further confirmed that the modified forms of PRP31 represented a covalent modification of PRP31 with ubiquitin using the denaturing NiNTA-pull down assay and found that USP15 WT but not inactive $USP15^{C269A}$ led to deubiquitination of PRP31 in the cell (Figure 2B). We then confirmed the interaction between PRP31 and USP15 with immunoprecipitation (Figure 2C). To examine whether PRP31 interacts directly with USP15, glutathione beads immobilized with a GST-tagged DUSP-UBL domain of USP15 was incubated with PRP31, which was synthesized with the *in vitro* transcription/translation (IVT/T) in the absence or presence of the SART3 HAT domains. As shown in Figure 2D, the DUSP-UBL domain of USP15 did not interact with PRP31. However, the DUSP-UBL domain of USP15 interacted with PRP31 in the presence of SART3 (Figure 2D) indicating that the interaction between PRP31 and USP15 was indirect but mediated by SART3.

Because SART3 is involved in the regulation of pre-mRNA splicing by recruiting the substrate PRP3 to USP4 (19), we considered the possibility of SART3 serving as a substrate targeting factor of USP15 as well. Initially, we examined the interaction between SART3 and PRP31. As shown in Figure 2E, we found that SART3 interacted with PRP31 by immunoprecipiation. To determine which region is required for the interaction between SART3 and PRP31, truncated mutants of SART3 were overexpressed. The interaction analysis with the truncated mutants of SART3 revealed that amino acids 120–286 in the HAT-N

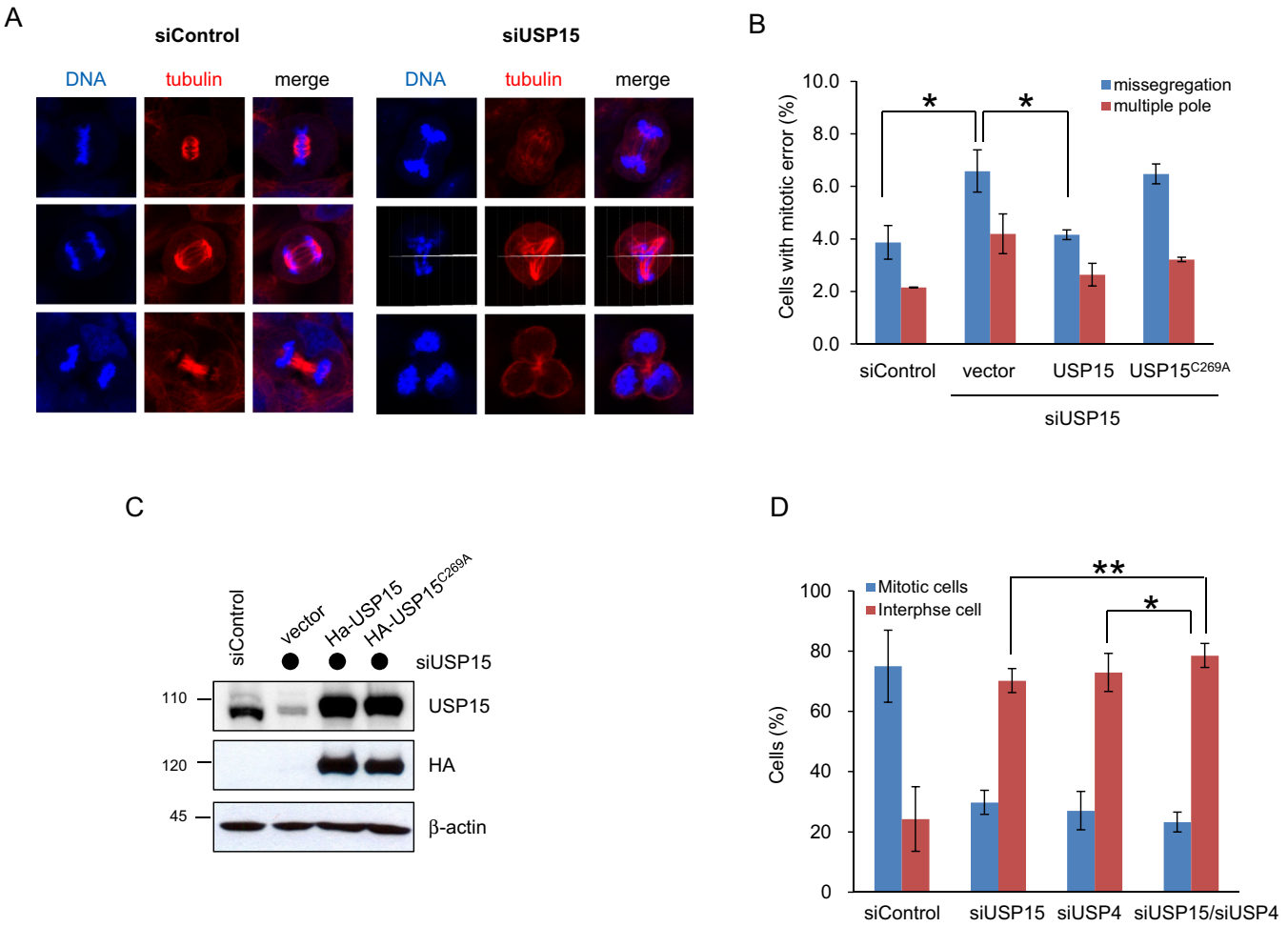

Figure 1. USP15 is required for proper chromosome segregation. (**A**) Mitotic spindle defects and chromosome missegregation in USP15 depleted cells. HeLa cells were transfected with control siRNA or USP15 siRNA-1 and immunostained with anti-β-tubulin-Cy3^{TM} (Sigma) monoclonal antibody. The nucleus was counterstained with DAPI. The images were acquired with a confocal microscope. (**B**) The activity of USP15 is required for the control of mitosis. HeLa cells were transfected with control siRNA or siRNA-1 against the 3′-untranslated region (UTR) of USP15 and stained as described in (A). The number of mitotic cells with errors in chromosome segregation or spindle formation was counted at 40X magnification with a fluorescence microscope. When indicated, cells were also transfected with vectors encoding siRNA-resistant USP15 or the catalytically inactive USP15^{C269A}. The data are shown as the mean ± S.D. from three independent experiments ($n = 3$; >500 cells per experiment; paired t-test $^{*}P < 0.05$). (**C**) The depletion of USP15 by siRNA was rescued by a vector encoding siRNA-resistant USP15. Cells were prepared as described in (B) and cell lysates were immunoblotted with anti-USP15 and anti-HA. (**D**) Co-depletion of USP15 and USP4 showed a synergistic effect in the mitotic defect. HeLa cells were transfected with USP15 siRNA, USP4 siRNA, or both of them. Forty-eight hours after the transfection, cells were treated with 100 nM taxol, and 24 h later, the percentage of cells arrested prior to mitosis (blue bar) and the number of cells unable to maintain a spindle checkpoint arrest (red bar) were determined. Data are shown as the mean ± S.D. from three independent experiments ($n = 3$; >500 cells per experiment; paired t-test $^{*}P < 0.05$, $^{**}P < 0.01$).

domain of SART3 were required for the interaction with PRP31 (Figure 2F). To investigate whether this interaction is direct, we generated PRP31-N domain (residues 1–333) and PRP31-C domain (residues 85–499) proteins based on the stabilities of the proteins for ITC measurements. The SART3 HAT domains did not interact with the PRP31-N domain whereas the PRP31-C domain had a significant endothermic-binding curve (Supplementary Figure S6A). The one-site binding analysis of the data yields an n of 1.07 and K_D of 5.16 μM. These data indicate that the SART3 HAT-N domain and PRP31-C domain are required for the interaction (Supplementary Figure S6B).

Next, we questioned the cellular localization of SART3, PRP31 and USP15. By performing immunofluorescence of HeLa cells transfected with these genes, we found that SART3 localized only in the nucleus whereas USP15 localized in both the nucleus and cytoplasm (Supplementary Figure S7A). Consistent with our recent study (26) co-expression of SART3 with USP15 led to the nuclear translocation of USP15, which suggests that SART3 has a significant effect on USP15 localization. This is in line with the report by Long *et al.* in which overexpression of SART3 enhanced localization of USP15 to the nucleus (27). Conversely, PRP31 and SART3 were colocalized in the nucleus (Supplementary Figure S7B). We then examined the localization of PRP31 and USP15 when cells were coexpressed with PRP31 and USP15. PRP31 localized in the nucleus and USP15 localized in the cytoplasm, shown in Figure 2G (upper panel), indicating that PRP31 itself did not have any direct effect on USP15 localization. However, the over-

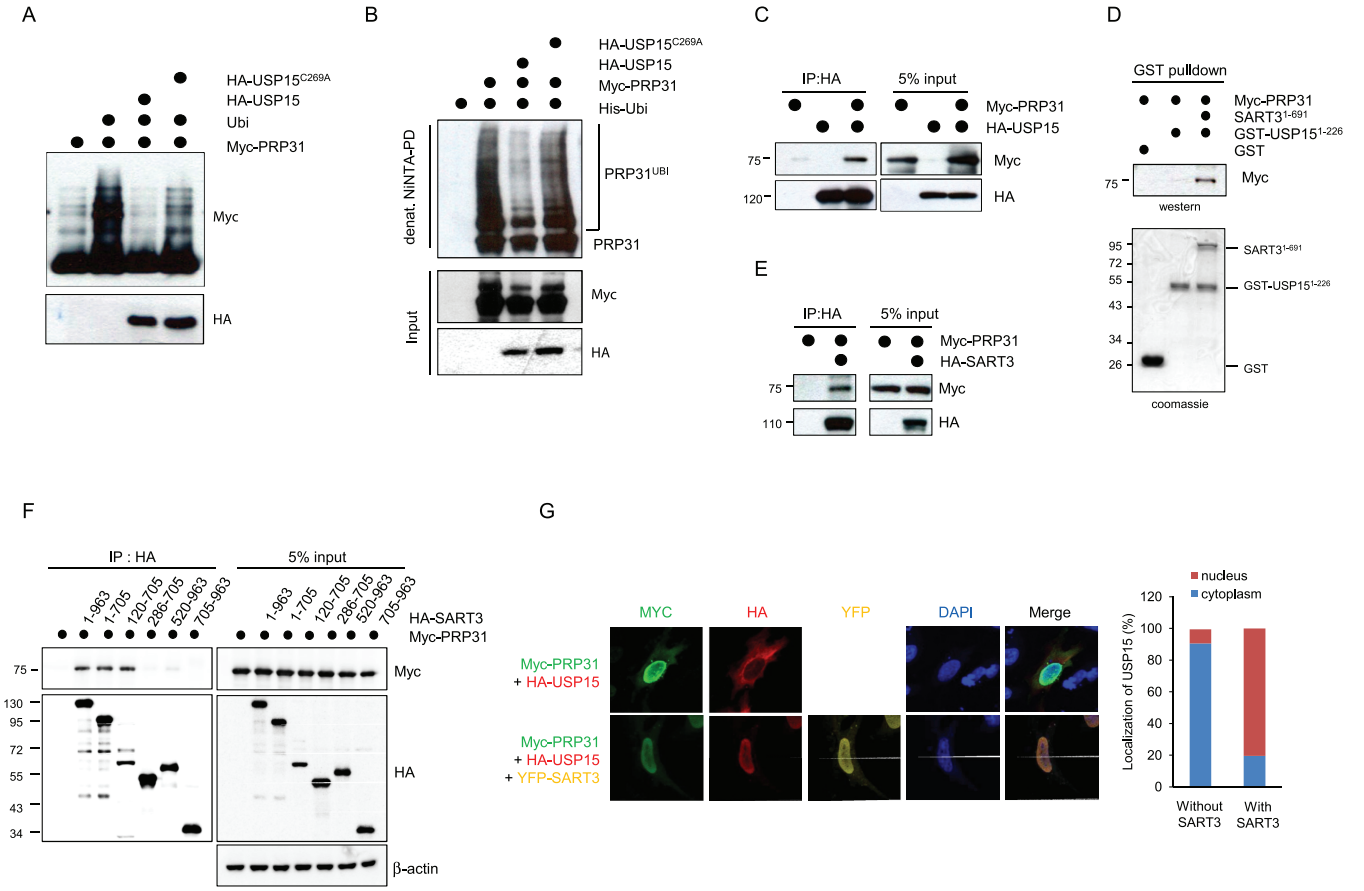

Figure 2. USP15 deubiquitinates PRP31. (**A**) Expression of ubiquitin triggers the modification on PRP31 in HeLa cells. Myc-PRP31 was coexpressed with ubiquitin and either USP15 or USP15^{C269A} in HeLa cells and was analyzed for modifications by anti-Myc western blotting. (**B**) USP15 deubiquitinates PRP31 in cells. Myc-PRP31 was coexpressed with His-ubiquitin together with USP15 or USP15^{C269A}, and covalently modified proteins were purified on NiNTA-agarose under denaturing conditions. Ubiquitinated PRP31 was detected by anti-Myc antibodies. (**C**) USP15 binds to PRP31 in cells. HA-USP15 and Myc-PRP31 were coexpressed in HeLa cells and purified on HA-agarose. Coprecipitated Myc-PRP31 was immunoblotted with anti-Myc antibodies. (**D**) PRP31 interacts with USP15 through SART3. Control GST or GST-USP15$^{1-226}$ was immobilized on glutathione beads and incubated with *in vitro* transcribed and translated Myc-PRP31 in the presence or absence of purified SART3$^{1-691}$. Bound proteins were separated in SDS-PAGE and detected by western blotting and Coomassie staining. (**E**) SART3 binds PRP31 in cells. HA-SART3 and Myc-PRP31 were coexpressed in HeLa cells and purified on HA-agarose. Coprecipitated Myc-PRP31 was immunoblotted with anti-Myc antibodies. (**F**) SART3 interacts with PRP31 through HAT-N domain. HeLa cells were transfected with Myc-PRP31 and HA-tagged truncations of SART3. HA-tagged truncations of SART3 were purified on HA-agarose, and coprecipitating PRP31 was detected by anti-Myc antibodies. (**G**) SART3 triggers the colocalization of USP15 and PRP31. HeLa cells were transfected with HA-USP15 and Myc-PRP31 in the absence or presence of YFP-SART3. The cells were immunostained with anti-HA and anti-Myc antibodies followed by Alexa488-conjugated anti-rabbit antibodies and Alexa546-conjugated anti-mouse antibodies. The nucleus was stained with DAPI. The intracellular localization of Myc-PRP31 (green), HA-USP15 (red) and YFP-SART3 (yellow) was analyzed by confocal microscopy. The percentage of USP15 expressing cells in the cytoplasm (blue bars) or nucleus (red bars) were quantitatively analyzed when cells were co-transfected with or without SART3.

expression of SART3 induced the nuclear localization of USP15, consequently leading to colocalization of USP15 with PRP31 (Figure 2G, lower panel). Additionally, the quantitative analysis clearly showed that the translocation of USP15 into the nucleus is dependent on SART3 (Figure 2G, right graph). Together, these data indicate that SART3 serves as a substrate targeting factor which recruits USP15 to its substrate PRP31.

PRP19 ubiquitinates PRP31

Subsequently, we searched for the E3 ligase which catalyzes the ubiquitination of PRP31. One strong candidate is the PRP19 complex (NTC), which consists of 30 proteins and forms an integral part of the spliceosome (2), and Prp19 has already been reported as an E3 ligase for PRP3 during USP4 mediated deubiquitination (19). We tested whether the PRP19 can ubiquitinates other spliceosomal proteins. As shown in Supplementary Figure S5, the overexpression of PRP19 strongly triggered the ubiquitination of PRP31 (Figure 3A) and PRP4 (Supplementary Figure S5). On the other hand, ubiquitination of PRP8 at the C-terminal by PRP19 was not as significant and PRP4B kinase and USP39 were not ubiquitinated by PRP19. Ubiquitinated PRP31 by PRP19 was reversed by USP15 WT, while the inactive mutant USP15^{C269A} did not show any effect (Figure 3B). The interaction between PRP31 and PRP19 was additionally confirmed by immunoprecipitation (Figure 3C), however, the interaction between the two was not direct (data not shown). These data suggest that PRP19 modifies sev-

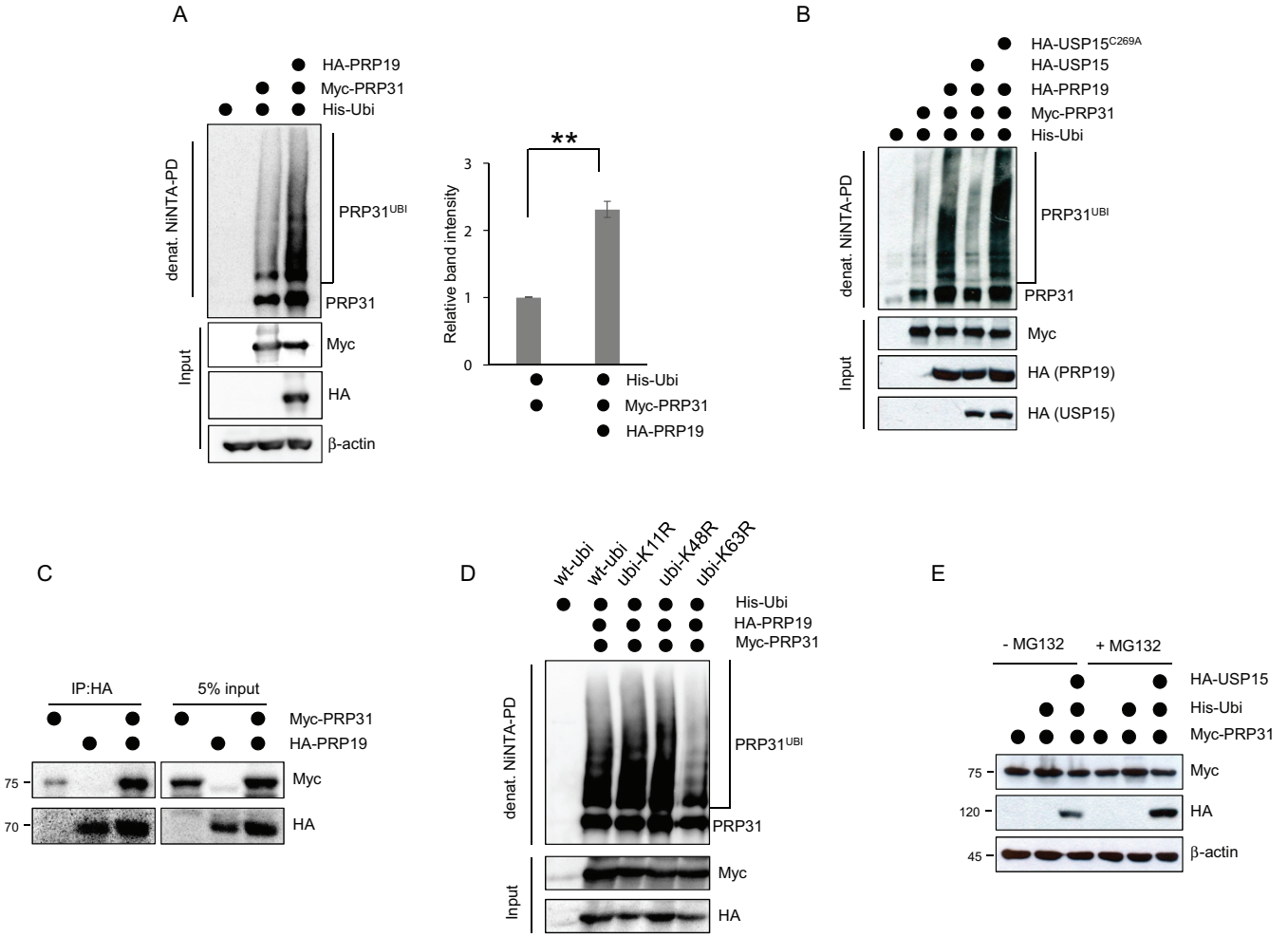

Figure 3. PRP19 ubiquitinates PRP31. (**A**) Expression of PRP19 triggers the ubiquitin modification on PRP31 in cells. Myc-PRP31 was expressed with His-ubiquitin in the absence or presence of PRP19, and covalently modified proteins were purified on NiNTA-agarose under denaturing conditions. Ubiquitinated PRP31 was detected by anti-Myc antibodies. Intensity of ubiquitinated PRP31 bands from western blotting was quantified and analyzed. The data are shown as the mean ± S.D. from three independent experiments ($n = 3$; paired t-test $^{*}P < 0.05$, $^{**}P < 0.01$). (**B**) USP15 counteracts the ubiquitination by PRP19. Myc-PRP31 was coexpressed with His-ubiquitin and PRP19 in the presence or absence of USP15. Covalently modified proteins were purified on NiNTA-agarose under denaturing conditions, and ubiquitinated Myc-PRP31 was detected by anti-Myc antibodies. (**C**) PRP19 interacts with PRP31 in cells. HeLa cells were transfected with HA-PRP19 and Myc-PRP31 as indicated. HA-tagged PRP19 was purified on HA-agarose, and coprecipitated PRP31 was detected by anti-Myc antibodies. (**D**) PRP19 promotes the modification of PRP31 with K63-linked ubiquitin chains in cells. Myc-PRP31 and PRP19 were coexpressed in HeLa cells, as indicated. The coexpression was performed in the presence of His-wt-ubiquitin, His-ubi-K11R (which has Lys11 mutated to Arg11), His-ubi-K48R (which has Lys48 mutated to Arg48) or His-ubi-K63R (which has Lys63 mutated to Arg63). Ubiquitin conjugates were purified on NiNTA-agarose under denaturing conditions, and ubiquitinated PRP31 was detected by anti-Myc antibodies. (**E**) Ubiquitination of PRP31 does not promote proteasomal degradation of PRP31. Myc-PRP31 was co-expressed with ubiquitin and USP15 in HeLa cells. The cells were treated with either DMSO (control) or MG132 (10 μM) for 4 h. Cell lysates were immunoblotted with anti-Myc antibodies, and β-actin was used as a loading control.

eral components of the U4/U6.U5 tri-snRNP complex, and PRP31 in particular is regulated by reversible ubiquitination by PRP19 and USP15.

To determine the functional role of the reversible ubiquitination of PRP31, we analyzed the chain specificity of PRP31 using ubiquitin mutants in which a Lys residue that is used for ubiquitin chain formation was replaced by an Arg residue. PRP19 failed to ubiquitinate PRP31 in the presence of K63R ubiquitin mutants, even though there was no changes in K11R or K48R mutants overexpressed cells compared to control (Figure 3D). Since the K63-ubiquitin chain usually does not associate with proteasomal degradation (15), we examined whether deubiquitination by USP15 has any effect on the cellular level of PRP31. Proteasome inhibitor MG132 did not show any alteration in the abundance of the PRP31 level (Figure 3E). This suggests that ubiquitination and deubiquitination of PRP31 are modiied by K63-linked chains in a nonproteolytic manner.

USP15 shows substrate preference for PRP31

Next, we examined by Ni-NTA pull-down assay whether USP15 has any cross reactivity with USP4 and found that ubiquitination of PRP31 was efficiently disassembled by USP15 but not by USP4 (Figure 4A). PRP3 was deubiquitinated by USP4 consistent with a previous report but

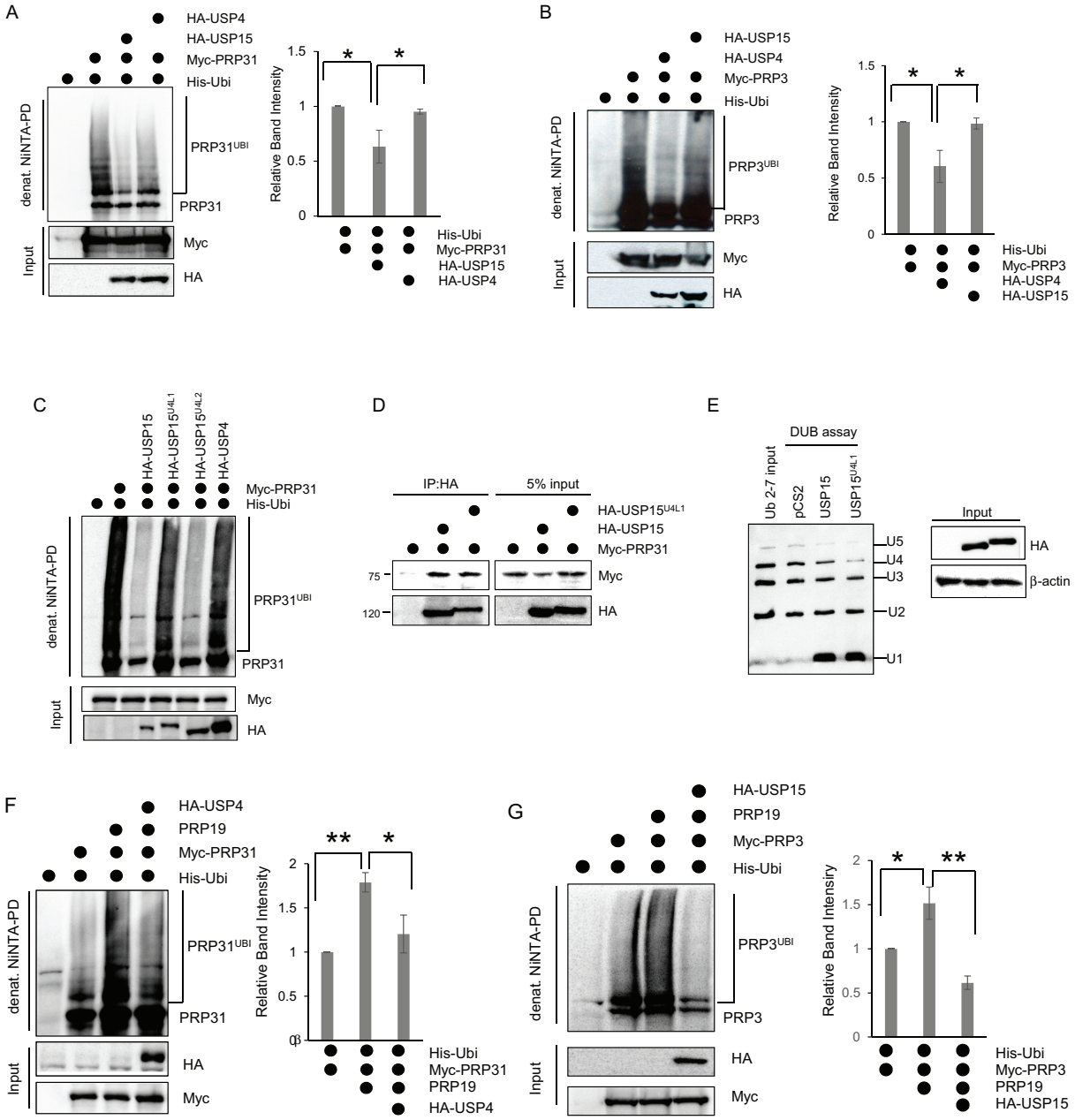

Figure 4. USP15 shows substrate preference for PRP31. (**A**) PRP31 is not deubiquitinated by USP4. Myc-PRP31 was expressed with His-ubiquitin, and either USP15 or USP4, and covalently modified proteins were purified on NiNTA-agarose under denaturing conditions. Ubiquitinated PRP31 was detected by anti-Myc antibodies. Intensity of ubiquitinated PRP31 bands from western blotting was quantified and analyzed. The data are shown as the mean ± S.D. from three independent experiments ($n = 3$; paired t-test $^*P < 0.05$). (**B**) PRP3 is not deubiquitinated by USP15. Myc-PRP3 was expressed with His-ubiquitin, and either USP15 or USP4, and covalently modified proteins were purified on NiNTA-agarose under denaturing conditions. Ubiquitinated PRP3 was detected by anti-Myc antibodies. Intensity of ubiquitinated PRP3 bands from western blotting was quantified and analyzed. The data are shown as the mean ± S.D. from three independent experiments ($n = 3$; paired t-test $^*P < 0.05$). (**C**) USP15 shows substrate preference through the linker 1 region. Myc-PRP31 was coexpressed with His-ubiquitin, and USP15, USP4, or swap mutants, USP15^{U4L1} and USP15^{U4L2}. Covalently modified proteins were purified on NiNTA-agarose under denaturing conditions and ubiquitinated Myc-PRP31 was detected by anti-Myc antibodies. (**D**) USP15^{U4L1} interacts with PRP31. HeLa cells were transfected with HA-USP15 or USP15^{U4L1} and Myc-PRP31 as indicated. HA-tagged USP15 was purified on HA-agarose and coprecipitated PRP31 was detected by anti-Myc antibodies. (**E**) USP15 and USP15^{U4L1} show similar activity in the cleavage of ubiquitin chains. Cells lysates overexpressed with pCS2 vector, HA-USP15 or HA-USP15^{U4L1} were purified on HA-agarose. Precipitated beads were incubated with K63-linked ubiquitin chains (UB_{2-7}, Boston Biochem) at 30°C for 90 min. The reactions were stopped and detected by anti-ubiquitin antibodies. (**F**) PRP31 is deubiquitinated by USP4 in the presence of PRP19. Myc-PRP31 was expressed with His-ubiquitin, PRP19 and USP4, and covalently modified proteins were purified on NiNTA-agarose under denaturing conditions. Ubiquitinated PRP31 was detected by anti-Myc antibodies. Intensity of ubiquitinated PRP31 bands from western blotting was quantified and analyzed. The data are shown as the mean ± S.D. from three independent experiments ($n = 3$; paired t-test $^*P < 0.05$, $^{**}P < 0.01$). (**G**) PRP3 is deubiquitinated by USP15 in the presence of PRP19. Myc-PRP3 was expressed with His-ubiquitin, PRP19 and USP15, and covalently modified proteins were purified on NiNTA-agarose under denaturing conditions. Ubiquitinated PRP3 was detected by anti-Myc antibodies. Intensity of ubiquitinated PRP3 bands from western blotting was quantified and analyzed. The data are shown as the mean ± S.D. from three independent experiments ($n = 3$; paired t-test $^*P < 0.05$, $^{**}P < 0.01$).

not by USP15 (Figure 4B). To identify the region that is responsible for the substrate recognition, we compared the sequences. The comparison suggested that two linker regions (Supplementary Figure S8) may have a role in the substrate recognition because sequence similarity of these regions is lower than others. The linkers 1 and 2 of USP15, which are a variable region compared to USP4, were replaced by those of USP4, respectively (referred to as $USP15^{U4L1}$ and $USP15^{U4L2}$ hereafter) (Supplementary Figure S8). $USP15^{U4L2}$ deubiquitinated PRP31 similar to USP15, but $USP15^{U4L1}$ did not although $USP15^{U4L1}$ had no effect on the interaction with PRP31 (Figure 4C and D). We examined further whether the enzymatic activity of $USP15^{U4L1}$ is hampered. USP15 and $USP15^{U4L1}$ were overexpressed and then purified on HA agarose. Immunoprecipitated USP15 and $USP15^{U4L1}$ were incubated with K63-linked ubiquitin chains. The results show that $USP15^{U4L1}$ was able to disassemble K63-linked ubiquitin chains, and the activity was comparable to USP15 (Figure 4E). These data suggest that the linker 1 region is important for the substrate recognition of USP15.

DUBs are known to be regulated by not only substrate recruitment but also by multiple mechanisms such as DUB recruitment factors, substrate-mediated regulation, activity modulation by external factors, post translational modifications and so on (30). Therefore, we investigated whether USP15 retains its substrate preference in the presence of E3 ligase. When PRP31 was ubiquitinated by PRP19, PRP31 was deubiquitinated by USP4 (Figure 4F). PRP3 was deubiquitinated by USP15 in the presence of PRP19 (Figure 4G). These findings suggest that USP15 deubiquitinates PRP3 as well as PRP31 when they are ubiquitinated by E3 ligase although USP15 may have more preference for PRP31.

USP15 and USP4 form a complex with SART3

Since SART3 serves as a substrate targeting factor for both USP15 and USP4 and the substrates for the two DUBs are closely related, we tested whether these three proteins form a complex. We found that USP15 interacts with both overexpressed (Figure 5A) and endogenous USP4 (Figure 5B). To examine whether USP15 interact with USP4 directly, we first carried out an ITC experiment using the DUSP-UBL domains of the two proteins. As shown in Supplementary Figure S9A, there was no binding between the two. We further investigated the possibility of USP15 interacting with other parts of USP4 using a GST-pull down assay. However, when full length USP4 synthesized with IVT/T was used, there was no binding (Supplementary Figure S9B) suggesting that the interaction between USP15 and USP4 is indirect. Next we considered the possibility of SART3 functioning as a platform for the two proteins, since SART3 is a direct interactor of both USP15 and USP4. Consistent with our prediction, SART3 interacted with endogenous USP4 and USP15 (Figure 5C). To examine the effect of endogenous SART3, the interaction between USP4 and USP15 was examined by immunoprecipitation after depletion of SART3 using siRNA. The depletion of SART3 hampered the interaction between USP15 and USP4 (Figure 5D and E). We next examined whether SART3 forms a complex with USP15 and USP4 simultaneously using sequential immunoprecipitation. As shown in the first IP of Figure 6A, SART3 and USP4 were retained by USP15 immunoprecipitation. In the second IP using anti-HA beads after elution with FLAG peptides, USP4 was still retained in the SART3 complex (Figure 6A, second IP). To present more direct evidence of a USP15–SART3–USP4 ternary complex formation, we overexpressed three differently tagged interacting partners (HA-SART3, Myc-USP4 and Flag-USP15) and lysates were fractionated by gel filtration with a Superdex 200 10/300 column and compared to a molecular weight marker. The molecular weight of SART3, USP4 and USP15 is about 110, 109 and 112 kDa, respectively, and SART3 is known to occur as a dimer in the cell (26,29). As shown in Figure 6B, HA-SART3 was present in many fractions with a corresponding molecular weight higher than 200 kDa; however, Myc-USP4 and Flag-USP15 appeared mostly in the fractions between 13 and 17. In the immunoprecipitation by anti-HA agarose using these fractions, the three proteins were co-precipitated in fraction 14, and the corresponding molecular weight was ∼440 kDa (Figure 6C). Taken together, the gel filtration analyses confirmed that USP15–SART3–USP4 made a complex in the cell. Moreover, we found that USP15 and USP4 deubiquitinated substrates PRP31 and PRP3 simultaneously (Figure 6D). These findings suggest SART3 binds to both USP15 and USP4, and this may lead to deubiquitination of PRP31 and PRP3 simultaneously.

We then examined whether complex formation has any effect on the enzymatic activity. USP15 was purified on HA agarose in the presence of SART3 WT or $SART3^{705–963}$ and then incubated with K63-linked ubiquitin chains. Figure 6E shows that USP15 disassembled the K63-ubiquitin chains well; however, there was no big difference with or without SART3 (Figure 6E compare lanes 3 and 4). It is likely that endogenous SART3 exists, and it already forms a complex with USP15 in the cell. However, the activity decreased when SART3 was mutated because it could not form a complex with USP15 and USP4. These data suggest that complex formation of USP15 and USP4 stimulates the enzymatic activity of USP15 and possibly USP4.

USP15-SART3-USP4 complex facilitate ubiquitin dependent regulation of RNA splicing

Ubiquitination and deubiquitination of the spliceosomal proteins are involved in the spliceosome activation through the regulation of the interaction between the spliceosomal proteins (11,19). It has been shown that the ubiquitin modification of PRP3 by USP4 and PRP19 regulates the interaction with U5 component PRP8 and is important for the assembly and stability of the U4/U6.U5 tri-snRNP complex (19). Being similar to USP4, the depletion of USP15 results in mitotic defects as seen in Figure 1, we investigated whether USP15 has any effect on the pre-mRNA splicing. The abundance of mature mRNA and pre-mRNA of Bub1 and α-tubulin, which are spindle checkpoint components, in USP4 or USP15 depleted cells was determined by qRT-PCR with primers spanning exon-junctions or primer pairs annealing to an exon and its neighboring intron. Consistent with our previous study (19), the loss of USP4 reduced

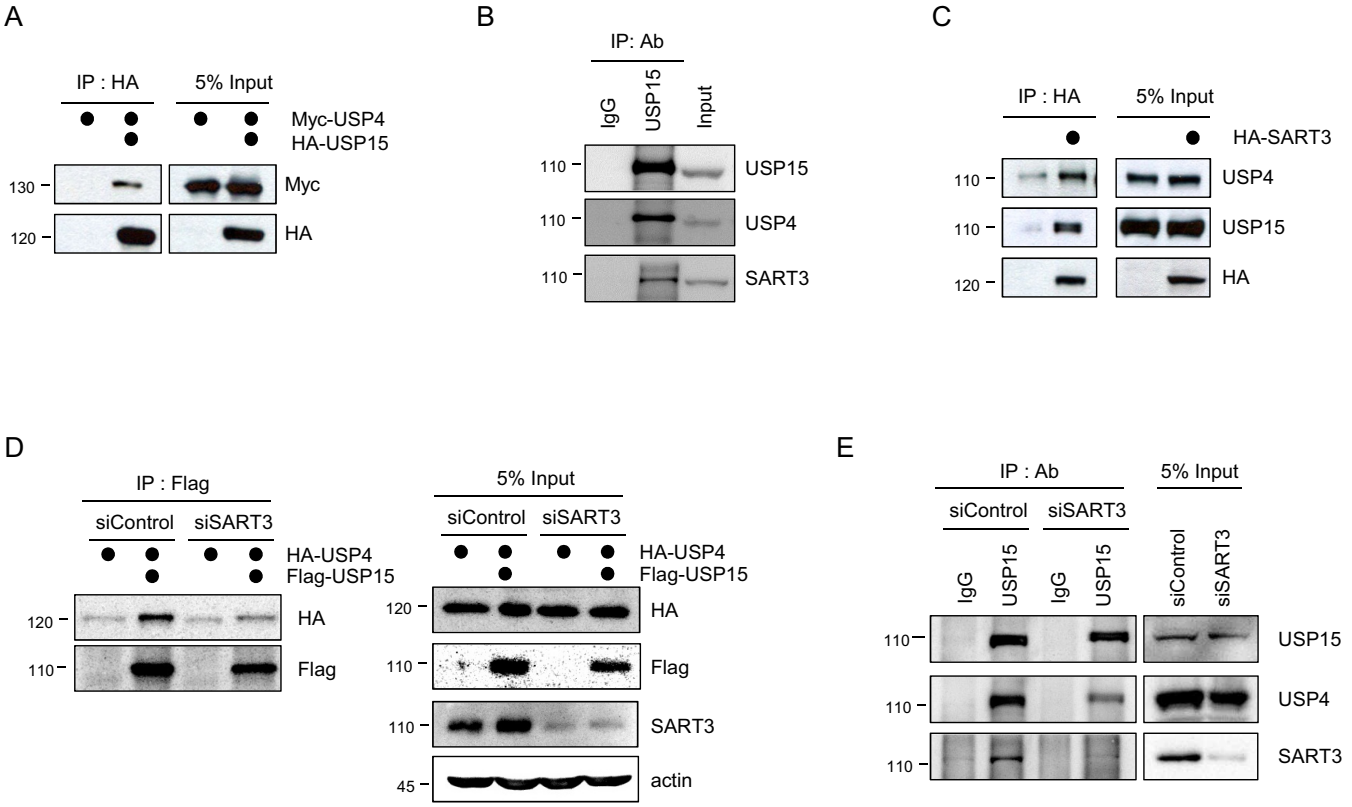

Figure 5. SART3 binds USP4 and USP15. (**A**) USP15 interacts with USP4 in cells. HeLa cells were transfected with Myc-USP4 and HA-USP15. HA-USP15 was purified on anti HA-agarose, and coprecipitating Myc-USP4 was detected by anti-Myc antibodies. (**B**) Endogenous USP15 coprecipitates with endogenous USP4 and SART3. Endogenous proteins in HeLa cells were precipitated with control IgG or anti-USP15 antibodies, and coprecipitated proteins were detected by anti-USP15, anti-USP4 or anti-SART3 antibodies. (**C**) SART3 binds USP4 and USP15 in cells. HA-SART3 transfected into HeLa cells was purified on HA-agarose, and coprecipitated proteins were detected by anti-USP4 or anti-USP15 antibodies. (**D**) The interaction between overexpressed USP15 and USP4 decreases in the depletion of SART3. HeLa cells were transfected with control siRNA or SART3 siRNA, and then transfected with HA-USP4 and Flag-USP15 after 24 h of siRNA transfection. HeLa cells were purified on Flag-agarose, and coprecipitated proteins were detected by anti-HA or anti-Flag antibodies. (**E**) The interaction between endogenous USP15 and USP4 decreases in the depletion of SART3. HeLa cells were transfected with control siRNA or SART3 siRNA and endogenous proteins in HeLa cells were precipitated with control IgG or anti-USP15 antibodies. Coprecipitated proteins were detected by anti-USP15, anti-USP4 or anti-SART3 antibodies.

the mRNA splicing of Bub1 and α-tubulin. Only the spliced mature mRNAs of Bub1 and α-tubulin but not their pre-mRNAs were downregulated by the depletion of USP15 (Figure 7A). In contrast, the mRNA level of H2AX, which does not possess any introns, did not change by the depletion of USP15. This result implies that USP15 is required to ensure the efficiency of splicing, at least for a few mRNAs in cells, which is required for the regulation of chromosome segregation.

To investigate whether the role of USP15 in mRNA splicing is related with ubiquitination and deubiquitination of PRP31, we examined the interaction between PRP31 and PRP8 in the presence or absence of ubiquitin because PRP8, which is a component of the U5 snRNP, is the acceptor of the ubiquitin chain regulating the assembly and disassembly of the U4/U6.U5 tri-snRNP complex (11,19). PRP31 interacted with the JAMM domain of PRP8 which was slightly increased in the presence of ubiquitin (Figure 7B). Moreover, addition of PRP19 increased the interaction between PRP31 and JAMM domain of PRP8 (Figure 7B). And then we examined whether deubiquitination by USP15 have an effect on the interaction. The addition of USP15 eliminated the interaction between PRP31 and the PRP8 JAMM domain, and co-overexpression of USP15 and USP4 accelerated this dissociation (Figure 7C). These results suggest that the interaction between PRP31 and PRP8 is dependent on the ubiquitination status of PRP31, and this interaction could possibly regulate the stabilization of the U4/U6.U5 tri-snRNP complex.

DISCUSSION

It is well known that the formation of the U4/U6.U5 tri-snRNP complex of spliceosome requires massive remodeling and the post-translational modifications as well as their reversibility of core components have been recognized as driving forces for the spliceosome dynamics (1,3,31). However, the detailed molecular mechanisms of how these modifications of spliceosomal proteins contribute to the assembly and disassembly of the U4/U6.U5 tri-snRNP complex are not fully understood. Therefore, the discovery of new post-translational modifications of the spliceosome would provide new regulatory mechanisms for spliceosome activation.

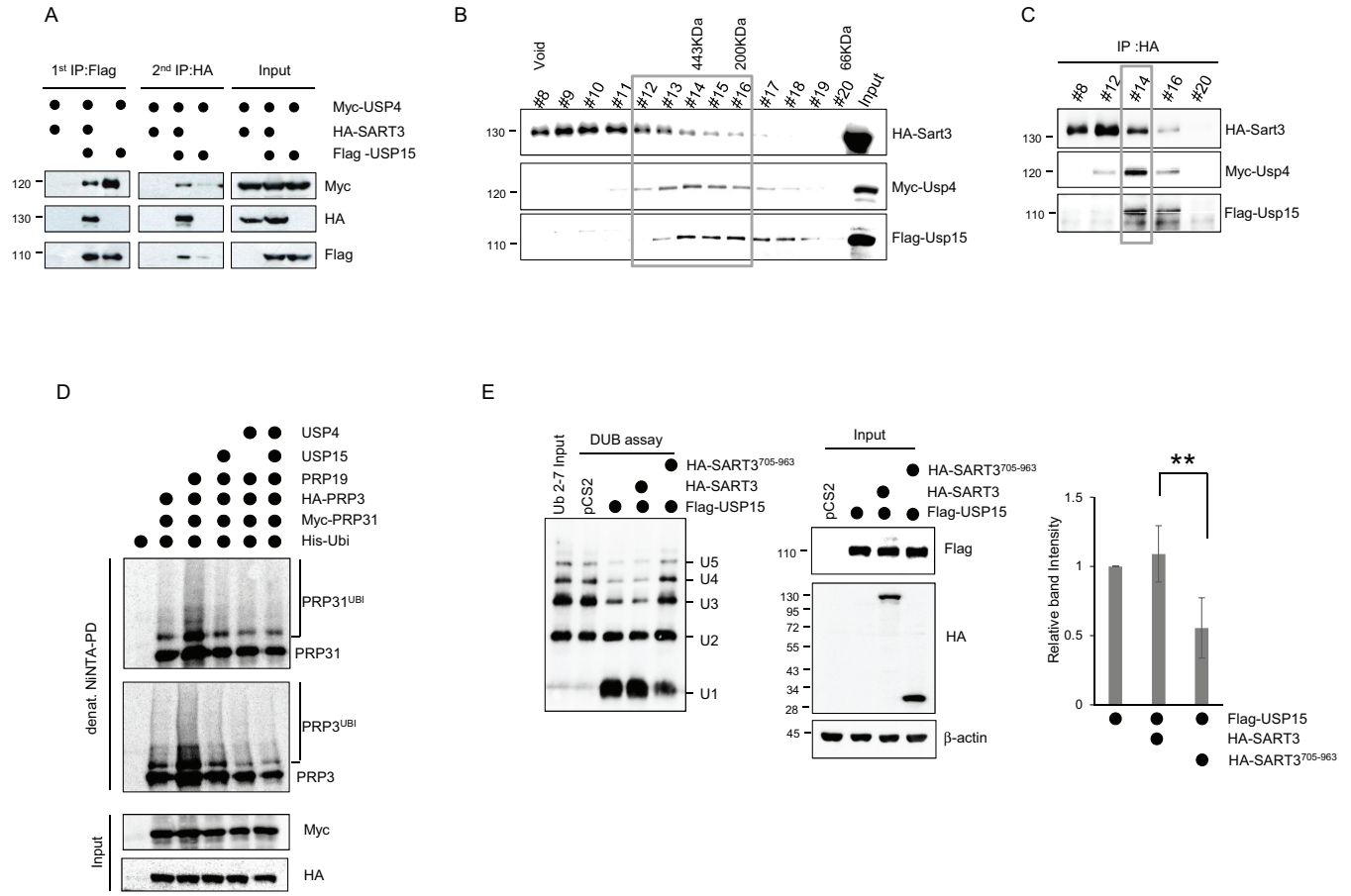

Figure 6. USP4 and USP15 form a complex with SART3. (**A**) USP15, USP4 and SART3 form a complex in the cell. For sequential IP, cell lysates overexpressed with HA-SART3, Flag-USP15 and Myc-USP4 were first purified on Flag-agarose. After elution with FLAG peptides, eluted samples were immunoprecipitated with anti-HA agarose. Coprecipitated proteins were detected by western blotting. (**B**) Cell lysates overexpressed with HA-SART3, Flag-USP15, and Myc-USP4 were fractionated by gel filtration with a Superdex 200 16/60 column (GE Healthcare Life Sciences). Molecular weight markers with a range of 66 000–443 000 daltons for size calibration were indicated. All fractions were analyzed by western blotting. (**C**) Fractions 8, 12, 14, 16 and 20 were immunoprecipitated with anti-HA agarose. Coprecipitated proteins were detected by western blotting. (**D**) USP15 and USP4 simultaneously deubiquitinate PRP3 and PRP31 modified by PRP19. HA-PRP3 and Myc-PRP31 were coexpressed with His ubiquitin, PRP19, and either USP15, USP4, or both of them. Covalently modified proteins were purified on NiNTA-agarose under denaturing conditions. Ubiquitinated PRP31 and PRP3 were detected by anti-Myc or anti-HA antibodies, respectively. (**E**) DUB complex is more active in cleavage of ubiquitin chains. Cells lysates overexpressed with Flag-USP15, and either HA-SART3 or HA-SART3$^{705\text{-}963}$ were first purified on Flag-agarose. After elution with FLAG peptides, eluted samples were incubated with K63-linked ubiquitin chains ($UB_{2\text{-}7}$, Boston Biochem) at 30°C for 90 min. The reactions were stopped and detected by anti-ubiquitin antibodies. Left lane indicates Ub2–7 input. Intensity of monoubiquitin versus ubiquitin 2–5 chains from western blotting was quantified and analyzed. The data are shown as the mean ± S.D. from three independent experiments ($n = 3$; paired t-test $^{**}P < 0.01$).

The PRP19 complex has been known to be required for the stable association of U5 and U6 snRNP after the dissociation of U4 snRNP for quite some time (61). But, it is only recent that it has an E3 ligase activity, and PRP3 is identified as the first substrate (19). The PRP19 complex may well ubiquitinate other spliceosomal proteins, and here we identify PRP31 and PRP4 as additional substrates. Our data show that ubiquitination of PRP31 increases its affinity towards the JAMM domain of U5 component PRP8, and conversely the addition of USP15 attenuates the interaction between PRP31 and PRP8 through deubiquitination of PRP31. Since another post-modification of PRP31, namely phosphorylation by PRP4 kinase, is shown to be required for the assembly of the tri-snRNP complex (14), and the depletion of PRP31 results in the accumulation of the U4/U6 di-snRNP complex (62), post-translational modifications of PRP31 seem to be important in modulating the interactions in snRNP complexes during the catalytic cycle of the spliceosome. Similar to PRP3, the ubiquitinated PRP31 is expected to interact with the PRP8 JAMM domain (19). This domain lacks deubiquitinating activity (32), but is known to interact with ubiquitin conjugates, and its interaction is important for the assembly and disassembly of U4/U6.U5 tri-snRNP (11). PRP8 is known to regulate the Brr2 activity through the insertion of the C-terminal tail at the Jab1 domain into the Brr2's RNA binding tunnel to prevent premature U4/U6 unwinding (33). These all support the idea that PRP8 regulates the assembly and disassembly of the U4/U6.U5 tri-snRNP complex by the interaction with ubiquitinated proteins. Together with observations from other reports, our data suggest that modification

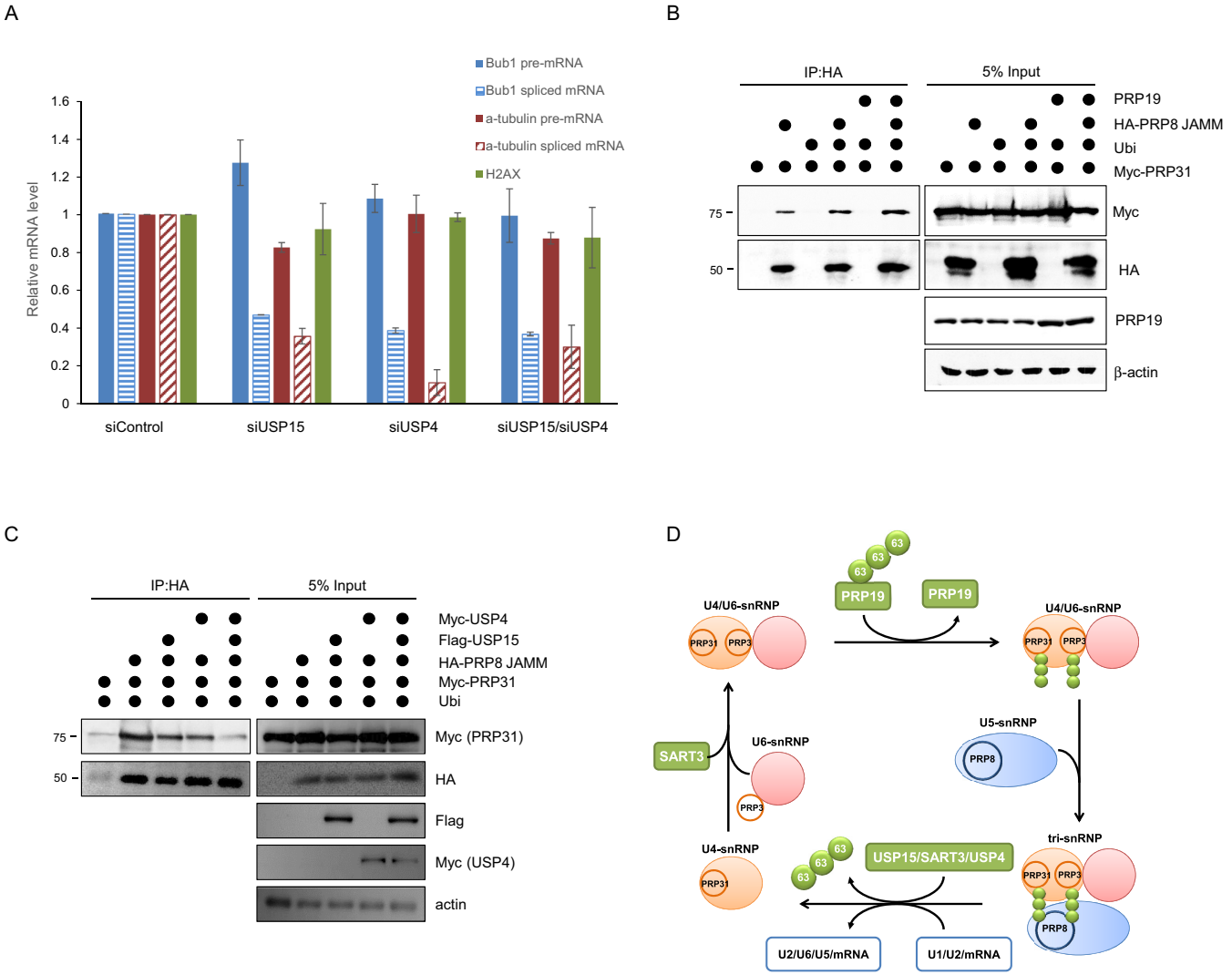

Figure 7. USP15 and USP4 facilitate ubiquitin dependent regulation of RNA splicing. (**A**) USP15 is required for the splicing of Bub1, a spindle checkpoint component. HeLa cells were transfected with siRNAs against USP15, USP4 or both of them. Forty-eight hours after transfection, cells were arrested in mitosis with nocodazole. The abundance of spliced mRNA and nonspliced pre-mRNA for the chromosome segregation regulated genes Bub1 and α-tubulin was determined by quantitative real time PCR. Primers spanning exon-junctions or annealing to an exon and its neighboring intron were used for qRT-PCR to detect the spliced mRNA and nonspliced pre-mRNA, respectively. H2AX, which does not possess any intron, was used as a control for proficient splicing Three independent qRT-PCR experiments were performed for each genes. (**B**) Ubiquitinated PRP31 is recognized by the JAMM domain of PRP8, which is a U5 spliceosome component. HA-tagged JAMM domain of PRP8 and Myc-PRP31 were overexpressed in HeLa cells with or without ubiquitin and PRP19. Proteins were purified on HA-agarose bead and coprecipitating PRP31 was detected by anti-Myc antibodies. (**C**) USP15 and USP4 induce the dissociation of PRP31 from the PRP8 JAMM domain. Myc-PRP31 and HA-PRP8 JAMM domain were overexpressed in HeLa cells in the presence of Flag-USP15 or Myc-USP4 or both of them. Coimmunoprecipitated PRP31 was detected by anti-Myc antibodies followed by purification on HA-agarose. (**D**) Working model of Usp15 and Usp4 mediated regulation of the spliceosome. Both Prp31 and Prp3, the U4/U6 snRNP components, are ubiquitinated by Prp19 with K63-linked ubiquitin chain. Ubiquitinated Prp31 and Prp3 in turn are recognized by U5 snRNP component Prp8 via its JAMM domain, and this may help the formation of the stabilized U4/U6.U5 tri-snRNP complex. Followed by successful docking of the U4/U6.U5 tri-snRNP complex at the spliceosome, Prp31 and Prp3 are deubiquitinated by the Usp15–Sart3–Usp4 complex, thereby decreasing the affinity towards Prp8 possibly resulting in the dissociation of the U4 snRNA from the tri-snRNP complex. Release of U4 snRNP facilitates pre-mRNA splicing of cell cycle regulatory genes, especially Bub1 and α-tubulin, by the active spliceosome complex.

of PRP31 by reversible ubiquitination possibly contributes to the remodeling of the U4/U6.U5 tri-snRNP complex.

Recent studies have shown that splicing regulators contribute to the precise splicing of cell cycle regulators. SON, a large Ser/Arg (SR)-related protein, acts as a coactivator for efficient RNA processing of cell cycle related genes with weak splice sites and controls cell cycle progression by coordinated regulation of RNA splicing (6). Other SR proteins such as SRSF2 and SRSF3 have a key role in cell cycle regulation and apoptosis in cancer cells (7,8). A single mutation of TgRRM1 arrests in the G1 phase by interaction with U4/U6.U5 tri-snRNP (9). Moreover, many genes undergo cell cycle dependent alternative splicing changes, and periodic alternative splicing is controlled by CLK1 (10). Several observations have shown more close connections between the spliceosome and mitosis. Depletion of spliceosome com-

ponents induces prometaphase delay and chromosome misalignment (34). Sister chromatid cohesion, which is an essential process for segregation of the chromosome, has been reported to be highly affected by the splicing machinery. Depletion of PRP19 (35) and PRP8 (36), which are required for the stabilization of the U4/U6.U5 tri-snRNP complex by PRP31 ubiquitination in our study result in premature loss of sister chromatid cohesion. Moreover, the direct function of the PRP19 complex in the mitotic spindle assembly has been reported (37). Although we showed a defect in the mRNA splicing of cell cycle related genes such as Bub1 and α-tubulin by the depletion of USP15, further studies on the link between ubiquitination and mRNA splicing will contribute to a better understanding of the regulation of mitosis by the spliceosome.

Among the one hundred or so DUBs identified in humans, some share similarities in their sequence and some in their function. For example, USP33 and USP20 (38), USP5 and USP13 (39), and USP12 and USP46 (40–42) share sequence homology with each other. USP33 and USP20 serve as regulators for the recycling and resensitization of the β2 adrenergic receptor (38), while USP12 and USP46 regulate histone deubiquitination (40). In the case of USP15 and USP4, in addition to being involved in many independent signaling pathways such as Parkin-mediated mitophagy (43), T-cell activation (44), Nrf2 (45), NF-κB (46), COP9 signalsome (47,48), histone H2B (27) and p53 (49), the two DUBs share functional similarities. For example, they are involved in the TGF-β signaling pathway; USP15 deubiquitinates and stabilizes TGF-β receptor I (50) or receptor-activated SMADs (51), while USP4 regulates the signaling pathway of TGF-β receptor I and is associated with a poor prognosis in breast cancer (52). They also are associated with RIG-I mediated antiviral signaling through the deubiquitination of E3 ligase Trim25 (53) or RIG-I (54,55), respectively. Our results here show yet another functional similarity of the two DUBs. However, this time the two appear to perform their functions as one complex. The knockdown of the two DUBs exhibited a slightly stronger phenotype for mitotic checkpoint bypass than the knockdown of each DUB alone (Figure 1D), and co-expression of the two increased the dissociation of PRP31 from PRP8 (Figure 7C) suggesting that the complex of USP15 and USP4 may be more active and efficient than each DUBs alone. It is worth noting that SART3 is crucial in forming the complex (Figure 5D), and the binding stoichiometry and affinity for the two DUBs are similar (26,29). Because SART3 forms a dimer (26), it could bind the two DUBs simultaneously, and may well serve as a platform for both USP15 and USP4 at the same time.

SART3 has been stated mostly as a U4/U6 recycling factor (24), but our data show that SART3 serves as a substrate targeting factor as well as acts as a platform for USP15 and USP4 binding. The relationship between these two roles is not clear yet, but it is quite possible that they are connected to each other. At the moment it is not clear yet when and how SART3 is recruited to the spliceosome, Makarov *et al.* reported the presence of SART3 in the spliceosomal intermediate complex, which is the complex prior to spliceosome activation, using proteomics analysis (56). This suggests that SART3 not only regulates U4/U6 recycling after splicing but also has a role before spliceosome activation. For the dual function of SART3, USP15 and USP4 might be able to dissociate from SART3 by some kind of modification on USP15 or USP4 themselves. Interestingly, mostly recently USP4 is reported to be auto-deubiquitinated to recruit CtIP and promote DNA repair (57,58), thus such modification of USP15 or USP4 could possibly regulate the interaction with SART3. An alternative model might be that the complex between USP15 and SART3 is constitutive, but USP15 or USP4 catalytic activity can be regulated post-translationally in a manner that is coupled to the status of spliceosome assembly/disassembly. This could be through a modification or adjusting the binding partner like other DUB's regulation (59,60).

In this study, we showed that USP15 has a substrate preference for PRP31. However, USP15 deubiquitinated PRP3 in the presence of E3 ligase. These data indicate that the substrate preference of USP15 decreases when the substrate is ubiquitinated by E3 ligase. Although we are not able to explain this phenomenon fully in this study, it is possible that the ubiquitinated substrate may have an effect on the catalytic activity of USP15. It has been reported that the catalytic activity of the USP4 catalytic domain alone is strongly inhibited by the slow dissociation of ubiquitin, while the presence of DUSP-UBL domains enhances ubiquitin dissociation hence promoting efficient turnover (22). USP15 shows a similar catalytic behavior as USP4 (22). Thus, substrate recruitment may well be the first regulating factor of USP15, and the ubiquitination status of the substrate can function as a next layer of regulation. We think that further studies are necessary to address the regulatory mechanism of USP15 in the future.

Here we found that a component of the U4 snRNP, namely PRP31, is modified with K63-linked ubiquitin chains by the PRP19 complex. Ubiquitinated PRP31 and PRP3, in turn, are recognized by the JAMM domain of U5 component PRP8, and this may help the formation of the stabilized U4/U6.U5 tri-snRNP complex. Deubiquitination of PRP31 and PRP3 by the USP15-SART3-USP4 complex decreases the affinity towards PRP8 and this regulation is important for the proper splicing of chromosome segregation related genes such as Bub1 and α-tubulin (Figure 7D). Based on our findings, we propose that both PRP31 and PRP3 are regulatory proteins in the dynamic protein–protein interactions of the spliceosome component through ubiquitination and deubiquitination. We hope our current findings advance the understanding of core post-translational modifications in the rearrangements of the spliceosome components.

SUPPLEMENTARY DATA

Supplementary Data are available at NAR Online.

FUNDING

National Research Foundation of Korea (NRF) grant funded by the Korea government (MSIP) [20110021713 and 2015R1A2A2A04005596]; R&D Convergence Program of NST (National Research Council of Science & Technology) of Republic of Korea [CAP-16-03-KRIBB]. Funding for

open access charge: National Research Foundation of Korea (NRF) grant funded by the Korea government (MSIP) [20110021713 and 2015R1A2A2A04005596]; R&D Convergence Program of NST (National Research Council of Science & Technology) of Republic of Korea [CAP-16-03-KRIBB].
Conflict of interest statement. None declared.

REFERENCES

1. Chen,W. and Moore,M.J. (2014) The spliceosome: disorder and dynamics defined. *Curr. Opin. Struct. Biol.*, **24**, 141–149.
2. Will,C.L. and Luhrmann,R. (2011) Spliceosome structure and function. *Cold Spring Harb. Perspect. Biol.*, **3**.
3. Hegele,A., Kamburov,A., Grossmann,A., Sourlis,C., Wowro,S., Weimann,M., Will,C.L., Pena,V., Luhrmann,R. and Stelzl,U. (2012) Dynamic protein–protein interaction wiring of the human spliceosome. *Mol. Cell*, **45**, 567–580.
4. Maeder,C. and Guthrie,C. (2008) Modifications target spliceosome dynamics. *Nat. Struct. Mol. Biol.*, **15**, 426–428.
5. Cooper,T.A., Wan,L. and Dreyfuss,G. (2009) RNA and disease. *Cell*, **136**, 777–793.
6. Ahn,E.Y., DeKelver,R.C., Lo,M.C., Nguyen,T.A., Matsuura,S., Boyapati,A., Pandit,S., Fu,X.D. and Zhang,D.E. (2011) SON controls cell-cycle progression by coordinated regulation of RNA splicing. *Mol. Cell*, **42**, 185–198.
7. Edmond,V., Merdzhanova,G., Gout,S., Brambilla,E., Gazzeri,S. and Eymin,B. (2013) A new function of the splicing factor SRSF2 in the control of E2F1-mediated cell cycle progression in neuroendocrine lung tumors. *Cell Cycle*, **12**, 1267–1278.
8. Kurokawa,K., Akaike,Y., Masuda,K., Kuwano,Y., Nishida,K., Yamagishi,N., Kajita,K., Tanahashi,T. and Rokutan,K. (2014) Downregulation of serine/arginine-rich splicing factor 3 induces G1 cell cycle arrest and apoptosis in colon cancer cells. *Oncogene*, **33**, 1407–1417.
9. Suvorova,E.S., Croken,M., Kratzer,S., Ting,L.M., Conde de Felipe,M., Balu,B., Markillie,M.L., Weiss,L.M., Kim,K. and White,M.W. (2013) Discovery of a splicing regulator required for cell cycle progression. *PLoS Genet.*, **9**, e1003305.
10. Dominguez,D., Tsai,Y.H., Weatheritt,R., Wang,Y., Blencowe,B.J. and Wang,Z. (2016) An extensive program of periodic alternative splicing linked to cell cycle progression. *Elife*, **5**.
11. Bellare,P., Small,E.C., Huang,X., Wohlschlegel,J.A., Staley,J.P. and Sontheimer,E.J. (2008) A role for ubiquitin in the spliceosome assembly pathway. *Nat. Struct. Mol. Biol.*, **15**, 444–451.
12. Mathew,R., Hartmuth,K., Mohlmann,S., Urlaub,H., Ficner,R. and Luhrmann,R. (2008) Phosphorylation of human PRP28 by SRPK2 is required for integration of the U4/U6-U5 tri-snRNP into the spliceosome. *Nat. Struct. Mol. Biol.*, **15**, 435–443.
13. McKay,S.L. and Johnson,T.L. (2010) A bird's-eye view of post-translational modifications in the spliceosome and their roles in spliceosome dynamics. *Mol. Biosyst.*, **6**, 2093–2102.
14. Schneider,M., Hsiao,H.H., Will,C.L., Giet,R., Urlaub,H. and Luhrmann,R. (2010) Human PRP4 kinase is required for stable tri-snRNP association during spliceosomal B complex formation. *Nat. Struct. Mol. Biol.*, **17**, 216–221.
15. Komander,D. and Rape,M. (2012) The ubiquitin code. *Annu. Rev. Biochem.*, **81**, 203–229.
16. Jin,L., Williamson,A., Banerjee,S., Philipp,I. and Rape,M. (2008) Mechanism of ubiquitin-chain formation by the human anaphase-promoting complex. *Cell*, **133**, 653–665.
17. Chen,Z.J. and Sun,L.J. (2009) Nonproteolytic functions of ubiquitin in cell signaling. *Mol. Cell*, **33**, 275–286.
18. Wertz,I.E. and Dixit,V.M. (2008) Ubiquitin-mediated regulation of TNFR1 signaling. *Cytokine Growth Factor Rev.*, **19**, 313–324.
19. Song,E.J., Werner,S.L., Neubauer,J., Stegmeier,F., Aspden,J., Rio,D., Harper,J.W., Elledge,S.J., Kirschner,M.W. and Rape,M. (2010) The Prp19 complex and the Usp4Sart3 deubiquitinating enzyme control reversible ubiquitination at the spliceosome. *Genes Dev.*, **24**, 1434–1447.
20. Kingston,R.E., Chen,C.A. and Okayama,H. (2003) Calcium phosphate transfection. *Curr. Protoc. Cell Biol.*, Chapter 20, Unit 20 23.
21. Maine,G.N., Li,H., Zaidi,I.W., Basrur,V., Elenitoba-Johnson,K.S. and Burstein,E. (2010) A bimolecular affinity purification method under denaturing conditions for rapid isolation of a ubiquitinated protein for mass spectrometry analysis. *Nat. Protoc.*, **5**, 1447–1459.
22. Elliott,P.R., Liu,H., Pastok,M.W., Grossmann,G.J., Rigden,D.J., Clague,M.J., Urbe,S. and Barsukov,I.L. (2011) Structural variability of the ubiquitin specific protease DUSP-UBL double domains. *FEBS Lett.*, **585**, 3385–3390.
23. Clerici,M., Luna-Vargas,M.P., Faesen,A.C. and Sixma,T.K. (2014) The DUSP-Ubl domain of USP4 enhances its catalytic efficiency by promoting ubiquitin exchange. *Nat. Commun.*, **5**, 5399.
24. Bell,M., Schreiner,S., Damianov,A., Reddy,R. and Bindereif,A. (2002) p110, a novel human U6 snRNP protein and U4/U6 snRNP recycling factor. *EMBO J.*, **21**, 2724–2735.
25. Trede,N.S., Medenbach,J., Damianov,A., Hung,L.H., Weber,G.J., Paw,B.H., Zhou,Y., Hersey,C., Zapata,A., Keefe,M. *et al.* (2007) Network of coregulated spliceosome components revealed by zebrafish mutant in recycling factor p110. *Proc. Natl. Acad. Sci. U.S.A.*, **104**, 6608–6613.
26. Park,J.K., Das,T., Song,E.J. and Kim,E.E. (2016) Structural basis for recruiting and shuttling of the spliceosomal deubiquitinase USP4 by SART3. *Nucleic Acids Res.*, **44**, 5424–5437.
27. Long,L., Thelen,J.P., Furgason,M., Haj-Yahya,M., Brik,A., Cheng,D., Peng,J. and Yao,T. (2014) The U4/U6 recycling factor SART3 has histone chaperone activity and associates with USP15 to regulate H2B deubiquitination. *J. Biol. Chem.*, **289**, 8916–8930.
28. Sowa,M.E., Bennett,E.J., Gygi,S.P. and Harper,J.W. (2009) Defining the human deubiquitinating enzyme interaction landscape. *Cell*, **138**, 389–403.
29. Zhang,Q., Harding,R., Hou,F., Dong,A., Walker,J.R., Bteich,J. and Tong,Y. (2016) Structural Basis of the Recruitment of Ubiquitin-specific Protease USP15 by Spliceosome Recycling Factor SART3. *J. Biol. Chem.*, **291**, 17283–17292.
30. Sahtoe,D.D. and Sixma,T.K. (2015) Layers of DUB regulation. *Trends Biochem. Sci.*, **40**, 456–467.
31. Wahl,M.C., Will,C.L. and Luhrmann,R. (2009) The spliceosome: design principles of a dynamic RNP machine. *Cell*, **136**, 701–718.
32. Bellare,P., Kutach,A.K., Rines,A.K., Guthrie,C. and Sontheimer,E.J. (2006) Ubiquitin binding by a variant Jab1/MPN domain in the essential pre-mRNA splicing factor Prp8p. *RNA*, **12**, 292–302.
33. Mozaffari-Jovin,S., Wandersleben,T., Santos,K.F., Will,C.L., Luhrmann,R. and Wahl,M.C. (2013) Inhibition of RNA helicase Brr2 by the C-terminal tail of the spliceosomal protein Prp8. *Science*, **341**, 80–84.
34. Valcarcel,J. and Malumbres,M. (2014) Splicing together sister chromatids. *EMBO J.*, **33**, 2601–2603.
35. Watrin,E., Demidova,M., Watrin,T., Hu,Z. and Prigent,C. (2014) Sororin pre-mRNA splicing is required for proper sister chromatid cohesion in human cells. *EMBO Rep.*, **15**, 948–955.
36. van der Lelij,P., Stocsits,R.R., Ladurner,R., Petzold,G., Kreidl,E., Koch,B., Schmitz,J., Neumann,B., Ellenberg,J. and Peters,J.M. (2014) SNW1 enables sister chromatid cohesion by mediating the splicing of sororin and APC2 pre-mRNAs. *EMBO J.*, **33**, 2643–2658.
37. Hofmann,J.C., Tegha-Dunghu,J., Drager,S., Will,C.L., Luhrmann,R. and Gruss,O.J. (2013) The Prp19 complex directly functions in mitotic spindle assembly. *PLoS One*, **8**, e74851.
38. Berthouze,M., Venkataramanan,V., Li,Y. and Shenoy,S.K. (2009) The deubiquitinases USP33 and USP20 coordinate beta2 adrenergic receptor recycling and resensitization. *EMBO J.*, **28**, 1684–1696.
39. Zhang,Y.H., Zhou,C.J., Zhou,Z.R., Song,A.X. and Hu,H.Y. (2011) Domain analysis reveals that a deubiquitinating enzyme USP13 performs non-activating catalysis for Lys63-linked polyubiquitin. *PLoS One*, **6**, e29362.
40. Cohn,M.A., Kee,Y., Haas,W., Gygi,S.P. and D'Andrea,A.D. (2009) UAF1 is a subunit of multiple deubiquitinating enzyme complexes. *J. Biol. Chem.*, **284**, 5343–5351.
41. Joo,H.Y., Jones,A., Yang,C., Zhai,L., Smith,A.D.t., Zhang,Z., Chandrasekharan,M.B., Sun,Z.W., Renfrow,M.B., Wang,Y. *et al.* (2011) Regulation of histone H2A and H2B deubiquitination and Xenopus development by USP12 and USP46. *J. Biol. Chem.*, **286**, 7190–7201.

42. Kee,Y., Yang,K., Cohn,M.A., Haas,W., Gygi,S.P. and D'Andrea,A.D. (2010) WDR20 regulates activity of the USP12 x UAF1 deubiquitinating enzyme complex. *J. Biol. Chem.*, **285**, 11252–11257.
43. Cornelissen,T., Haddad,D., Wauters,F., Van Humbeeck,C., Mandemakers,W., Koentjoro,B., Sue,C., Gevaert,K., De Strooper,B., Verstreken,P. *et al.* (2014) The deubiquitinase USP15 antagonizes Parkin-mediated mitochondrial ubiquitination and mitophagy. *Hum. Mol. Genet.*, **23**, 5227–5242.
44. Zou,Q., Jin,J., Hu,H., Li,H.S., Romano,S., Xiao,Y., Nakaya,M., Zhou,X., Cheng,X., Yang,P. *et al.* (2014) USP15 stabilizes MDM2 to mediate cancer-cell survival and inhibit antitumor T cell responses. *Nat. Immunol.*, **15**, 562–570.
45. Villeneuve,N.F., Tian,W., Wu,T., Sun,Z., Lau,A., Chapman,E., Fang,D. and Zhang,D.D. (2013) USP15 negatively regulates Nrf2 through deubiquitination of Keap1. *Mol. Cell*, **51**, 68–79.
46. Fan,Y.H., Yu,Y., Mao,R.F., Tan,X.J., Xu,G.F., Zhang,H., Lu,X.B., Fu,S.B. and Yang,J. (2011) USP4 targets TAK1 to downregulate TNFalpha-induced NF-kappaB activation. *Cell Death Differ.*, **18**, 1547–1560.
47. Huang,X., Langelotz,C., Hetfeld-Pechoc,B.K., Schwenk,W. and Dubiel,W. (2009) The COP9 signalosome mediates beta-catenin degradation by deneddylation and blocks adenomatous polyposis coli destruction via USP15. *J. Mol. Biol.*, **391**, 691–702.
48. Peth,A., Boettcher,J.P. and Dubiel,W. (2007) Ubiquitin-dependent proteolysis of the microtubule end-binding protein 1, EB1, is controlled by the COP9 signalosome: possible consequences for microtubule filament stability. *J. Mol. Biol.*, **368**, 550–563.
49. Zhang,X., Berger,F.G., Yang,J. and Lu,X. (2011) USP4 inhibits p53 through deubiquitinating and stabilizing ARF-BP1. *EMBO J.*, **30**, 2177–2189.
50. Eichhorn,P.J., Rodon,L., Gonzalez-Junca,A., Dirac,A., Gili,M., Martinez-Saez,E., Aura,C., Barba,I., Peg,V., Prat,A. *et al.* (2012) USP15 stabilizes TGF-beta receptor I and promotes oncogenesis through the activation of TGF-beta signaling in glioblastoma. *Nat. Med.*, **18**, 429–435.
51. Inui,M., Manfrin,A., Mamidi,A., Martello,G., Morsut,L., Soligo,S., Enzo,E., Moro,S., Polo,S., Dupont,S. *et al.* (2011) USP15 is a deubiquitylating enzyme for receptor-activated SMADs. *Nat. Cell Biol.*, **13**, 1368–1375.
52. Zhang,L., Zhou,F., Drabsch,Y., Gao,R., Snaar-Jagalska,B.E., Mickanin,C., Huang,H., Sheppard,K.A., Porter,J.A., Lu,C.X. *et al.* (2012) USP4 is regulated by AKT phosphorylation and directly deubiquitylates TGF-beta type I receptor. *Nat. Cell Biol.*, **14**, 717–726.
53. Pauli,E.K., Chan,Y.K., Davis,M.E., Gableske,S., Wang,M.K., Feister,K.F. and Gack,M.U. (2014) The ubiquitin-specific protease USP15 promotes RIG-I-mediated antiviral signaling by deubiquitylating TRIM25. *Sci. Signal.*, **7**, ra3.
54. Wang,L., Zhao,W., Zhang,M., Wang,P., Zhao,K., Zhao,X., Yang,S. and Gao,C. (2013) USP4 positively regulates RIG-I-mediated antiviral response through deubiquitination and stabilization of RIG-I. *J. Virol.*, **87**, 4507–4515.
55. Zhang,H., Wang,D., Zhong,H., Luo,R., Shang,M., Liu,D., Chen,H., Fang,L. and Xiao,S. (2015) Ubiquitin-specific protease 15 negatively regulates virus-induced type I interferon signaling via catalytically-dependent and -independent mechanisms. *Sci. Rep.*, **5**, 11220.
56. Makarov,E.M., Owen,N., Bottrill,A. and Makarova,O.V. (2012) Functional mammalian spliceosomal complex E contains SMN complex proteins in addition to U1 and U2 snRNPs. *Nucleic Acids Res.*, **40**, 2639–2652.
57. Wijnhoven,P., Konietzny,R., Blackford,A.N., Travers,J., Kessler,B.M., Nishi,R. and Jackson,S.P. (2015) USP4 auto-deubiquitylation promotes homologous recombination. *Mol. Cell*, **60**, 362–373.
58. Liu,H., Zhang,H., Wang,X., Tian,Q., Hu,Z., Peng,C., Jiang,P., Wang,T., Guo,W., Chen,Y. *et al.* (2015) The deubiquitylating enzyme USP4 cooperates with CtIP in DNA double-strand break end resection. *Cell Rep.*, **13**, 93–107.
59. Huang,O.W., Ma,X., Yin,J., Flinders,J., Maurer,T., Kayagaki,N., Phung,Q., Bosanac,I., Arnott,D., Dixit,V.M. *et al.* (2012) Phosphorylation-dependent activity of the deubiquitinase DUBA. *Nat. Struct. Mol. Biol.*, **19**, 171–175.
60. Yin,J., Schoeffler,A.J., Wickliffe,K., Newton,K., Starovasnik,M.A., Dueber,E.C. and Harris,S.F. (2015) Structural insights into WD-repeat 48 activation of ubiquitin-specific protease 46. *Structure*, **23**, 2043–2054.
61. Chan,S.P., Kao,D.I., Tsai,W.Y. and Cheng,S.C. (2003) The Prp19p-associated complex in spliceosome activation. *Science*, **302**, 279–282.
62. Schaffert,N., Hossbach,M., Heintzmann,R., Achsel,T. and Lührmann,R. (2004) RNAi knockdown of hPrp31 leads to an accumulation of U4/U6 di-snRNPs in Cajal bodies. *EMBO J.*, **23**, 3000–3009.